DOI : 10.5958/2277-8934.2026.00017.7 Vol 33 No 2, p 133-148

FROM DECEPTION TO DETECTION: MULTIMODAL DIAGNOSTIC IMAGING AND ELECTROMYOGRAPHIC ASSESSMENT OF COSMETIC TAMPERING IN CAMELS (*Camelus dromedarius*)

Waleed Elsayed Ahmed Ellawatty[1,*] and Margreet Voermans[2]

[1]Head of the Medical Imaging Department and the Chair of the Camel Tampering Detection Committee at Salam Camel Hospital-Salam Veterinary Group, Buraydah

[2]Sporthorsevet Consultant, Camel and Equine Surgeon and Sports Medicine Specialist, Al-Hofuf, Saudi Arabia

ABSTRACT

Cosmetic tampering in dromedary camels at beauty competitions remains inadequately documented. This comprehensive study evaluated 5,365 camels using integrated diagnostic imaging and electromyography to assess tampering prevalence and detection methods. One thousand and ninety-five camels (20.4%) showed cosmetic tampering, predominantly lip stretching, followed by subcutaneous air injection, nasal fillers, elevated testosterone, and lip binding, with less frequent cases of lip filler injection, nostril abscessation, ear cropping, nerve anaesthesia, and hump filler injection. Ultrasonography was the most sensitive diagnostic tool, discriminating normal from manipulated tissues by identifying hypoechoic or anechoic foci. Radiography revealed radiolucent areas in acute cases and soft tissue opacities with calcifications chronically, while CT imaging delineated tissue tearing, oedema, and hyperdense deposits. Infrared thermography showed thermal asymmetry in manipulated regions, and EMG demonstrated progressive muscle activity decline, with near-complete suppression in locally anaesthetised animals. Multimodal imaging combined with electrodiagnostic techniques reliably detected cosmetic tampering, with ultrasonography as the primary diagnostic tool while radiography, CT, infrared thermography, and EMG provided complementary assessment enabling differentiation between recent and chronic manipulations. This multimodal protocol constitutes a comprehensive diagnostic framework, in which each technique targets specific forms of cosmetic tampering, ensuring that the combined application minimises the likelihood of any manipulation or fraudulent practice remaining undetected. These findings highlight significant health and welfare risks, supporting the need for routine screening and regulatory enforcement at camel competitions to detect and regulate such unethical practices.

Key words: Computed tomography, cosmetic tampering, diagnostic imaging, dromedary camels, electromyography, radiography, thermography, ultrasonography

The tradition of evaluating camel beauty has its roots in Bedouin culture, where camels have long been valued not only for their utility but also for their aesthetic qualities. The practice evolved from informal gatherings where Bedouin tribes would showcase their finest animals to today's highly organised festivals, with the King Abdulaziz Camel Festival in Saudi Arabia emerging as one of the most prestigious events in the region (Ahmad *et al,* 2010). The festival includes camel beauty contests where camels are judged based on their physical appearance, including attributes like long, droopy lips and a shapely hump. However, the pursuit of winning has led to unethical practices, including the use of cosmetic enhancements such as Botox and fillers to alter the appearance of camels (Bieh *et al,* 2019). Recent years have witnessed growing concerns about artificial enhancement methods in camel beauty contests, not only due to their potential use in unfair competition, but also of their associated adverse health and welfare effects, including tissue damage, inflammation, functional impairment, and long-term structural alterations (Tharwat, 2025).

The Salam Veterinary Group (Salam Camel Hospital) has also taken a leading role in preserving the integrity of camel beauty competitions by developing and implementing the region's first comprehensive veterinary protocol for detecting

SEND REPRINT REQUEST TO WALEED ELSAYED AHMED ELLAWATTY email: waleedellawatty@yahoo.com/ wellawatty@svg.sa

all forms of cosmetic tampering. The present study employed using advanced diagnostic tools including X-rays, ultrasound, thermal imaging cameras, CT scans, blood tests for hormone analysis, and neurological diagnostic devices to accurately identify various forms of manipulation and unethical practices in dromedary camels.

Materials and Methods

Camel population

The research took place at Salam Veterinary Group's Camel Hospital, focusing on cases admitted from July 5, 2020, to February 5, 2026, to identify unlawful practices and alterations to camels to improve their appearance (Fig 1). A thorough evaluation was conducted on 5,365 dromedary camels (*Camelus dromedarius*), ranging in age from 2 months to 10 years and weighing between 100 and 650 kg, to assess these modifications. All cases were initially subjected to detailed visual clinical examination to detect any external abnormalities, including visible clinical signs suggestive of elevated testosterone levels, followed by assessment using diagnostic imaging modalities. Different camel breeds were included in the study, such as black camels (Majaheem) and coloured camels (Maghateer) which comprised Waddah (white), Homor (red-coated), Sofor (yellow-brown), Shaele (gray to brown-red), and Shageh (light or luminous-coated) camels. As a control group, 60 camels of different breeds, matched by age and weight and not subjected to any cosmetic enhancements, were examined concurrently.

Clinical and imaging examinations were conducted, and in cases requiring sedation for computed tomography (CT) scanning, camels were sedated using intravenous administration of xylazine (Bomazine 2%, BOMAC Laboratories Ltd., New Zealand) at a dose of 0.2 mg/kg IV (Al-Mubarak *et al,* 2008).

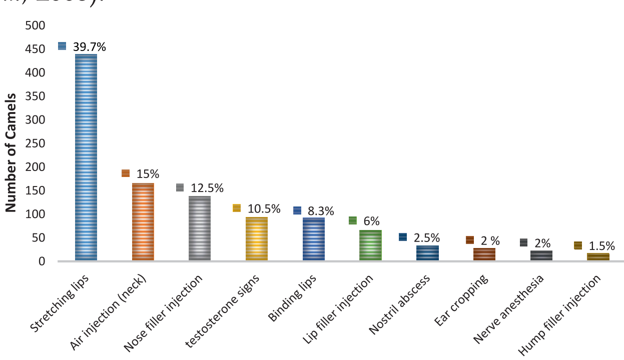

Fig 1. Distribution of different forms of tampering among examined camels (n = 1,095) from July 5, 2020, to February 5, 2026, expressed as numbers and percentages.

Radiographic Investigations

Radiographic examination of the head, neck and hump regions was carried out using Atomoscope HF400V portable x-ray unit (DLC Vet Pty Ltd., Japan).

Lateral views of the hump, head, and neck, along with dorso-ventral views of the head and neck, were obtained for all camels, with radiographic setting 76kVp, 1.6mAs, 15mA and a 70 cm focal film distance were used to examine all camels. All obtained radiographs were subjectively interpreted. Each radiograph was interpreted while blinded as to which camels received air injections in head and neck or not.

Computed Tomography Investigations

The CT examinations were conducted using the robot, also called EDAMIS (Equine Dual-Arm Multi-modality Imaging System), which was developed in the United States by Orimtech LTD. The robot was more than 3 metres tall and weighed almost 6 tonnes.

Prior to image acquisition, machine-specific calibration and warm-up protocols should be followed; this takes approximately 30 min. A fast calibration and tube warm-up should be performed on a daily basis only if the machine is to be used for scanning. It is preferable to maintain the temperature of the CT room at 20–28°C with humidity of 30–60%. A requirement of 7.1 kW peak heat output is necessary to support the equipment in the CT scanning room.

After the CT machine setup, the camels were loaded after immobilisation in sternal recumbency on Haico's adjustable height feature surgical table after slight sedation as mentioned before. A head collar was used substituted for a blindfolded rope or webbing halter to avoid metal image artefacts. Once the camel was sedated, the head and neck were extended onto a cradle to perform CT to avoid muscle overlap with placement of cushions under the body and neck to maintain alignment and avoid motion artefacts.

The area of clinical interest dictated the extent of the scan in the present study. For camel head and neck imaging, the starting point was starting from the mandibular ramus and scan caudally to the thoracic inlet (top of chest) to capture the common injection zones (lips, cheek, jawline, neck, ears and shoulder area). For hump assessment, scanning was extended over the dorsal thoracic region, encompassing the entire hump from its cranial to caudal margins to evaluate subcutaneous and adipose tissues.

Once the position of the scan was confirmed, the room was cleared of additional personnel, and the scan was commenced once the camel handler was safely positioned. CT images were obtained using the following parameters: cranial vision of image (V.V.F.), 3 s exposure time, 120 kV, 130 mA and 1-3 mm slice thickness and 3 mm image spacing. Best image quality for soft tissue was obtained by adjusting window widths and window levels. For visualising soft tissue lip structures, a soft-tissue window setting (window width, 1500; window level, 100) was used.

The scanner consists of two robotic arms and several cameras that register the camel's movements. The arms of the robot rotate around the blindfolded and sedated camel taking a series of images in as little as 30 seconds. These images were converted by a computer system into a detailed three-dimensional image, as in a conventional CT scan. The cameras allowed movement correction to be made. Mild movements were thus filtered out in order to guarantee razor-sharp image quality.

Ultrasonography Investigations

After positioning the camels in sternal recumbency, hand palpation of the lips, throat, hump, clitoris and skin region preceded the ultrasonographic examination for further identifying any abnormal structures or sounds. High-resolution ultrasound (MyLabTMOMEGA, Esaote S.P.A., Italy) was used for scanning. The ultrasound unit was equipped with 4 probes (microconvex 11R, 3.0– 11.0 MHz; linear T-shaped 50mm (appleprobe), 4.2– 15 MHz; and linear array probe, 10–22 MHz). The linear T-shaped and the linear array transducers were used for scanning the lips, throat, neck, clitoris and hump region. The examination was performed after applying alcohol then ultrasound gel to the scanning area. A fixed distance of about 5 mm between the area to scan and the probe was set. Both upper and lower lips were scanned from medial to lateral and from dorsal to ventral and the changes were stored and analysed. Both right and left sides of head and neck were scanned from the lower part of the head (below the jawline) to the thoracic inlet, Scanning the areas that are swollen or suspected of air injection, paying attention to any abnormal pockets or changes in tissue texture and the changes were stored and analysed. Images were acquired in B-mode and Colour Doppler at the maximum transmit frequency (18 MHz, harmonic), and a gain set to 45 and 60 dB of dynamic range.

Infrared Thermography Investigations

The thermographic camera used was a Hti-Xintai (China) (Infrared resolution 256x192, thermal sensitivity of 0. 07°C, temperature range of -20°C degrees to 550°C, automatic hot/cold detection). The infrared camera was also equipped with laser pointer, LaserSharp® Auto Focus for consistently in-focus images and laser distance meter that calculates distance to the target for precisely focused images and displays distance on screen. After cleaning the neck, lips, clitoris and hump region from any dirt, the thermographic measurements of all animals were taken with ambient temperature was minimum 6-17°C (11.5±4.7°C) and maximum 20-27°C (24.5±3.0°C) and relative humidity 26-80% (50.7±18.7%).

A period of 10-15 minutes was allowed for all animals before scanning for rest and to avoid 'stress-induced hyperthermia' (SIH) which is a common response to acute stress or to repeated stressing episodes. The thermographic camera was positioned perpendicularly at a distance of 0.2 metres from throat and neck area and the images were obtained in triplicate by a trained researcher. Thermographic profiles were analysed using Hti-Xintai® IR Image Tools software (China) where the experimental parameters and emissivity □ = 0.95 were assumed. After processing, maximum, minimum, and average temperature values of each animal's lips, hump, head and neck region were obtained. Abnormal or asymmetrical temperature distributions have been used as indicators of underlying problems with blood circulation or inflammatory responses.

EMG of the camel lips

ES (electric stimulation) was performed according to a standardised diagnostic protocol using biphasic multipulse trains of constant voltage generated by an intraoperative neurophysiological monitoring system (The Neuro-MEP-Micro, Ivanovo, Russia).

Two cable, colour coded red and black for disposable electrode with 2 Alligator clip - touch-proof (L 0.2 m, Russia) were mounted with 5 cm apart and parallel to each other on the upper and lower lips on each side and stimulation electrode with steel stimulation points (2.5 m) was applied to nerve supply at its emergence from infraorbital foramen and mental foramen at the upper and lower lip, respectively.

Multipulse ES was performed with 3 biphasic pulses per train (ppt), pulse width (pw) of 0.1 ms/phase and interpulse interval (ipi) of 1.0ms. The stimulation voltage was increased using a stepwise protocol: 0, 2, 4, 6, 8, V. At each voltage, transcranial stimulation was performed twice. The diagnostic MEP parameters were retrieved at 2, 4, 6 and 8 V respectively above motor threshold (MT). No further ES stimulations were added to the clinical diagnostic protocol for the present study.

When motor thresholds (MT) were reached for both muscle groups of lips, stimulation was continued to MT + 2 V or otherwise stopped at 8 V. At each occasion of stimulation, the motor responses were recorded for later retrieval of MEP (myogenic evoked potentials) amplitudes, MLTs (motor latency time) and waveform morphology.

Results

Camels under investigation tolerated the procedure as a number of well-trained assistants for camels were used during clinical and imaging using different devices to ensure the safety of the examiner and ease of the procedure. The average age of the camels ranged from 2 months to 10 years, and their weights ranged from 100 to 650 kg.

Out of a total of 5,365 examined camels, 4,903 were females and 462 were males. Among these, 1,095 camels (20.4%) including 906 females and 189 males were confirmed to exhibit various forms of tampering (Fig 1). The most prevalent form of tampering was lip stretching, recorded in 439 camels (39.7%). This was followed by air injection in the throat and neck region in 166 cases (15%), and nasal injection with filler materials in 138 camels (12.5%). On physical examination, visible clinical signs suggestive of elevated testosterone levels were identified in 94 camels (10.5%), including clitoral enlargement accompanied by a noticeable protrusion of the dulla, ranging from small to moderate size in female camels (Fig 18). While lip binding was identified in 92 cases (8.3%). Less frequently observed practices included lip injection with filler materials (66 camels, 6%), nostril abscessation as a complication from nasal injection with filler materials (33 camels, 2.5%), ear cropping (28 camels, 2%), nerve anaesthesia (22 camels, 2%), and hump injection with filler materials (17 camels, 1.5%). Notably, none of these abnormalities were detected in the control group.

Radiographic Investigations

In control groups, the skin, subcutaneous tissue and muscles of throat and neck region appeared with radiography examination appeared as light gray thin outer margin, medium gray band under skin and medium to dark gray homogeneous area, respectively (Fig 2). Radiographic findings of the examined camels detected air trapped in deeper tissues where air pockets in the acute stage, appeared as black radiolucent areas in the skin or subcutaneous tissues. These pockets showed up as spread in a diffuse and lacy pattern (Fig 3). While in advanced cases, after air absorption, X-rays revealed the presence of well-defined, round soft tissue opacities with calcifications seen as white specks in scarred areas in the X-ray. These can sometimes contained gas from secondary infection which indicted fluid collections and abscesses formation (Fig 4). Whereas, in most advanced and complicated cases the radiographic findings showed scar tissue (fibrosis) which appeared as whiter and radio-opaque due to its increased density and the throat area appeared denser on the X-ray (Fig 5).

Radiographic evaluation of the injected perinasal region by fillers in camels revealed variable soft tissue swelling corresponding to injected filler materials, which appeared as grayish areas with heterogeneous soft tissue density (Fig 6).

Radiographic assessment of the hump region demonstrated abnormal soft tissue changes consistent with the presence of exogenous filler materials. These changes were characterised by focal to multifocal areas of increased radiopacity relative to adjacent soft tissues, often exhibiting irregular margins and heterogeneous internal architecture. The injected materials produced nodular or diffuse radiodense

Fig 2. Radiograpic examination in control groups, the skin, subcutaneous tissue and muscles of throat and neck region-appeared as light gray thin outer margin, medium gray band under skin and medium to dark gray homogeneous area, respectively.

patterns, indicating variable distribution within the subcutaneous tissues (Fig 7). In some cases, these alterations were associated with contour irregularities and localised enlargement of the hump, reflecting cosmetic augmentation. In contrast, control animals exhibited homogeneous soft tissue opacity with no evidence of abnormal radiographic features.

Computed Tomography Investigations

On a CT scan, the normal dermis in the control group appeared as an isodense structure as illustrated in Fig 8. While in animals with stretched lips the tearing in tissues and oedema appeared hypodense areas within isodense structure of the dermis as seen in Fig 9, with formation of hyperdense structure appeared as bright white shades with white spots within soft tissue (Fig 10).

CT imaging of the lips and perinasal region in the examined camels revealed the presence of filler materials within the submucosal and subcutaneous tissues of the upper, lower lips and nasal bridge (rhinarium). These materials appeared as well-defined or slightly ill-defined hyperdense areas relative to the surrounding soft tissue, often forming nodular or elongated deposits. No involvement of the oral cavity or underlying musculature was observed.

A CT scan of a normal camel's cervical region skin in control group appeared as thin outer soft

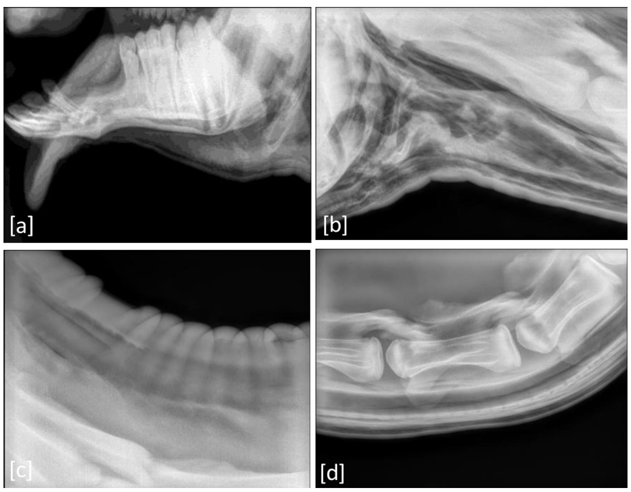

Fig 3. Radiographic findings of the camel's throat and neck region detected air trapped in deeper tissues where air pockets appeared as black radiolucent areas in the skin or subcutaneous tissues of lower mandible[a], throat[b], dorsal[c] and ventral[d] aspect of neck. These pockets showed up as spread in a diffuse and lacy pattern.

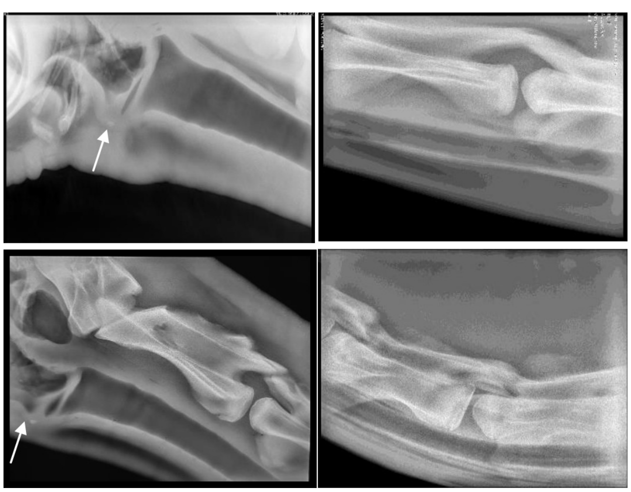

Fig 4. X-rays revealed in advanced cases, after air absorption, the presence of well-defined, round soft tissue opacities with corrugated skin and calcifications seen as white specks in scarred areas in the X-ray and the throat area appeared denser on the X-ray.

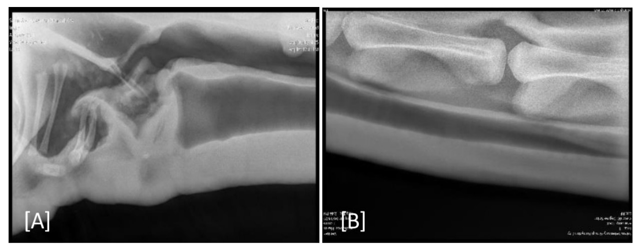

Fig 5. Radiographic findings in most advanced and complicated cases they showed whiter and radio-opaque increased density which indicates fibrosis at the throat[a] and neck area[b] appeared denser on the X-ray.

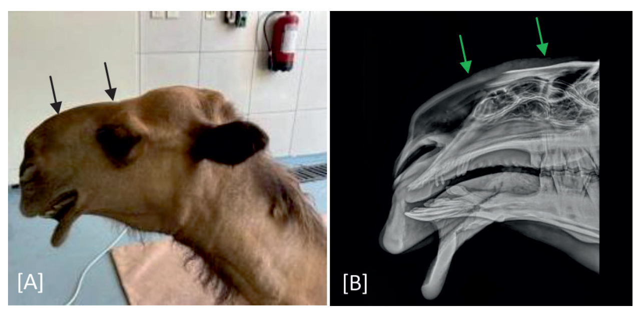

Fig 6. Enlargement of the perinasal area (black arrows) in a female camel due to injection of filler material (A). Image (B) shows a lateral radiographic view of the same camel, showing the gray-coloured injected filler material (green arrows) in the perinasal region.

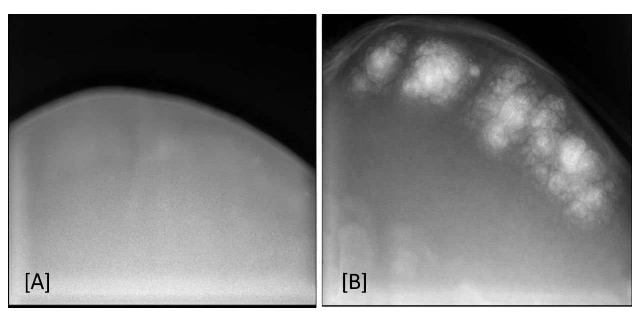

Fig 7. Lateral radiographic view of dromedary camel hump: (A) control animal showing homogeneous soft tissue density with normal hump contour; (B) demonstrating abnormal soft tissue opacity with nodular filler deposits and irregular contours.

tissue layer isodense to other soft tissues while fat appeared darker grey, with Hounsfield Units (HU) around -100 to -50. Homogenous with no air bubbles appeared in normal cases. Whereas the muscles (e.g., *sternocephalicus, brachiocephalicus, longus colli*) appeared light grey, uniform in texture with slightly higher HU than fat (~40–60 HU) and clearly separated by fascial planes (Fig 11). The injected camels on CT examination showed very low attenuation, black, irregularly distributed, non-encapsulated areas and typically measuring ~ -1000 Hounsfield Units (HU) with streaky or bubbly shape that follow the fascial planes, separating muscle bundles or collecting under the skin in the ventral, lateral, or caudal neck regions and can tracked cranially toward the mandible (Fig 12). The tissues appeared normal, aside from the air which may indicate that the injection was recent.

In some cases of injected camels found with increased soft tissue density compared to normal fat and fat planes become hazy or blurred which looked like a diffuse, cloudy or 'ground-glass' appearance — due to fluid accumulation and oedema formation (Fig 13). and the Hounsfield Units (HU) typically shift from normal fat values (-100 to -50 HU) to higher values (0 to +20 HU), depending on severity with less distinct muscular borders due to surrounding fluid and with thickened denser skin and subcutaneous layer and neck diameter appeared increased, irregular contours and asymmetry compared to camels in control groups.

CT imaging of the hump region demonstrated abnormal soft tissue alterations indicative of exogenous filler injection. These changes were characterised by focal and multifocal areas of increased attenuation compared to the surrounding adipose tissue, often exhibiting heterogeneous internal characteristics and irregular margins. The injected materials were frequently observed as nodular or diffusely distributed hyperattenuating

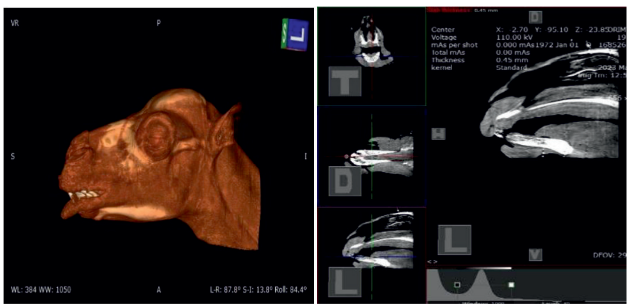

Fig 8. Computed tomography showed normal lips appeared as an isodense structure (gray shades) for a female camel.

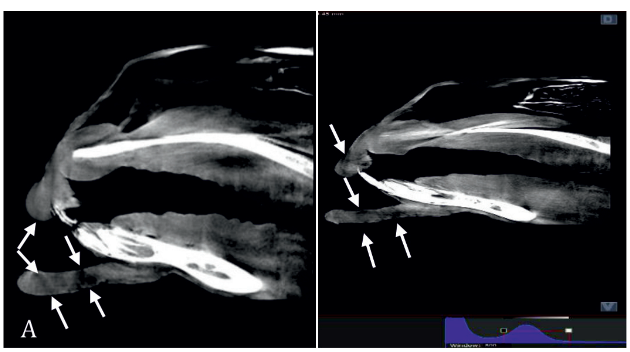

Fig 9. Computed tomography showed tearing tissue in stretched lips appeared as hypodenisity black shade areas (white arroaws) within normal isodense gray shade muscle of camel's lips.

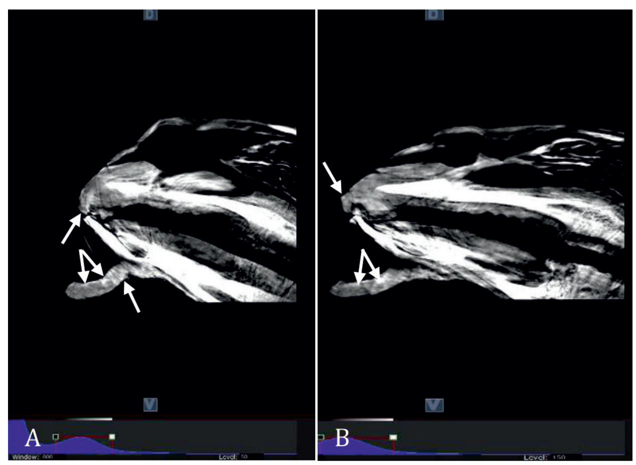

Fig 10. Computed tomography showed fibrosis in stretched lips appeared as hyper density lesion within normal isodense gray shade muscle of camel's lips.

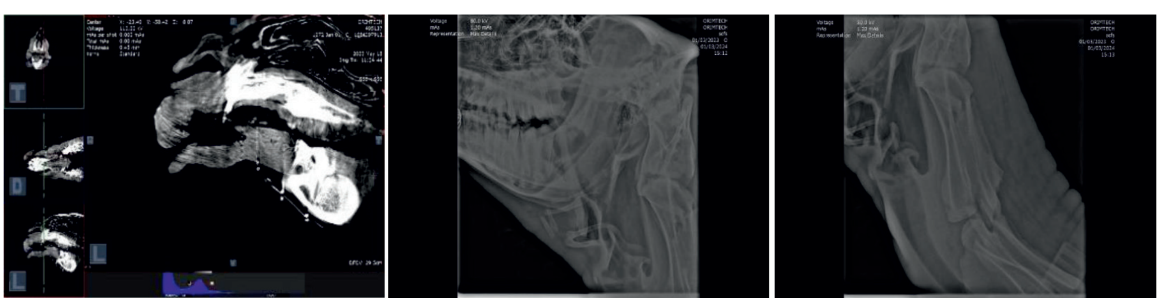

Fig 11. A CT scan of a normal camel's cervical region skin in control groups appeared as thin outer soft tissue layer isodense to other soft tissues while fat appeared darker grey, homogenous with no air bubbles in normal cases.

Fig 12. A CT examination of injected camels showed very low attenuation, black, irregularly distributed, non-encapsulated areas with bubbly shape that collecting under the skin in the ventral, lateral, or caudal neck regions and can tracked cranially toward the mandible (white arrow).

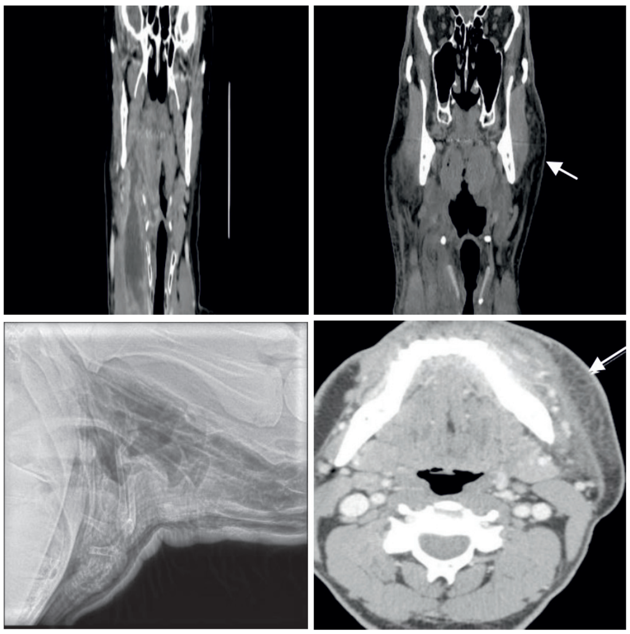

Fig 13. CT imaging revealed cervical cellulitis with increased soft tissue density compared to normal fat which looked like a diffuse, cloudy or 'ground-glass' appearancedue to fluid accumulation and oedema formation (white arrows).

deposits within the subcutaneous layer, disrupting the normal fat architecture (Fig 14). In some instances, these deposits were associated with structural distortion, including asymmetrical enlargement and contour deformities of the hump. In contrast, control animals showed uniform, low-attenuation adipose tissue with no evidence of focal lesions or structural abnormalities.

Ultrasonography Investigations

Ultrasonographic examination proved valuable for assessing the various cosmetic procedures performed on camels. Upon ultrasound, the normal dermis in the control groups appeared as a hyperechoic structure easily differentiated from the hypoechoic subcutaneous tissue. In camels with stretched lips, it was difficult to distinguish the subcutaneous tissue from the dermis. The stretched lips appeared anechoic and/or hypoechoic and was imaged as small or large, single or multiple areas of tissue tearing and oedema formation. In the injected lips, the filler materials appeared as areas of low echogenicity, producing heterogeneous images with increased overall lip thickness. In cases of lip binding, the lip tips presented either as isoechoic areas with a hypoechoic rim or as hypoechoic areas with an echogenic centre. In the perinasal region, the filler material appeared as hypoechoic or anechoic foci within the soft tissues as illustrated in Fig 15.

In control groups, the skin and subcutaneous tissue of head and neck region appeared with ultrasound examination as a layered, bright hyperechoic line with dark hypoechoic fat beneath. While neck muscles layers showed up as relatively homogeneous, striated, hypoechoic structures. With

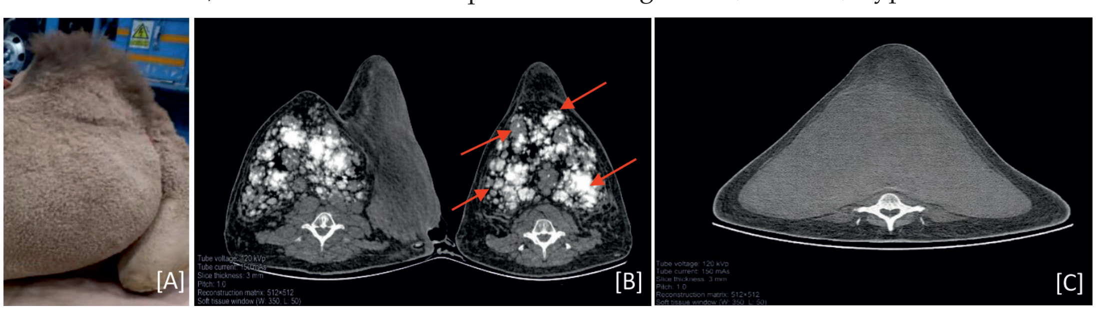

Fig 14. CT imaging of the camel hump(A); revealed abnormal soft tissue changes consistent with exogenous filler injection, characterised hyperattenuating subcutaneous deposits with irregular, heterogeneous appearance disrupting normal fat architecture and causing hump deformity (red arrow) (B), compared to normal uniform adipose tissue in controls (C).

the ultrasound examination, the injected air in throat and neck region appeared as bright hyperechoic areas where air is trapped under the skin. In some cases, Aair typically showed as small pockets with well-defined borders and created dirty shadowing artifacts appeared as lines behind the air pockets but in others, the ultrasound imaging identified multiple small bubbles which appeared in a cluster and gives off a grainy pattern on the scan which indicate recent air injection in these sites whereas in advanced cases, the scanned images showed dark, anechoic areas which indicated fluid buildup in the tissues and oedema formation, which could be present after air absorption as shown in Fig 16.

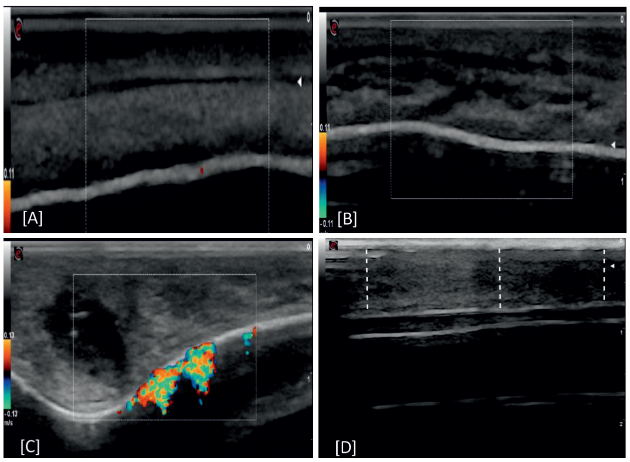

Fig 15. Ultrasonographic findings of cosmetic procedures in camels: (A) control showing normal hyperechoic dermis and hypoechoic subcutaneous tissue; (B) stretched lips showing anechoic/hypoechoic areas with tissue tearing and oedema; (C) injected lips showing hypoechoic, heterogeneous filler deposits with increased lip thickness; (D) perinasal region showing hypoechoic/anechoic filler foci within soft tissues (white dots).

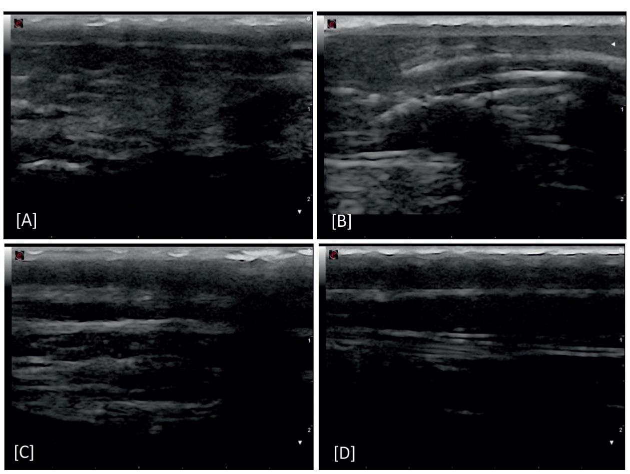

Fig 16. Ultrasonography demonstrates; (A) control showing layered hyperechoic cervical skin with underlying hypoechoic fat and homogeneous, striated hypoechoic muscles; (B) air injection showing hyperechoic subcutaneous pockets; (C) Ssmall air pockets with dirty shadowing or clustered echogenic bubbles indicating recent injection; (D) advanced cases showing anechoic areas consistent with fluid accumulation and oedema.

Ultrasonographic examination of the camel hump revealed the presence of injected filler materials within the subcutaneous and fatty tissues. These materials appeared as hypoechoic or anechoic nodules, often heterogeneous in echotexture, causing localised thickening of the hump. The filler deposits were irregular in shape and distributed along the subcutaneous fat, without involvement of the underlying musculature. No vascular flow was detected within the injected areas compared to hump of control group (Fig 17).

Ultrasound examination of the normal female camel clitoris revealed a small, well-defined, homogeneous structure with moderate echogenicity and uniform surrounding tissues, while Doppler imaging showed normal vascular flow. Whereas ultrasonography of the clitoris in hormonally treated female camels revealed pronounced enlargement, appearing as a moderately echogenic, homogeneous structure with well-defined margins, causing protrusion and mild thickening of the surrounding soft tissues causing protrusion, whereas in some cases, the clitoral tissue appeared disrupted or partially absent on ultrasound, presenting as irregular, heterogeneous hypoechoic to anechoic areas with ill-defined margins and localised thinning of the surrounding tissues (Fig 18).

Infrared Thermography Investigations

Infrared thermography (IRT) proved useful for detecting injected filler substances in the lips and for assessing stretched or elongated lips. The injected sites appeared darker than the surrounding tissue, reflecting relatively higher temperatures compared to healthy, non-injected lip tissue. In contrast, stretched

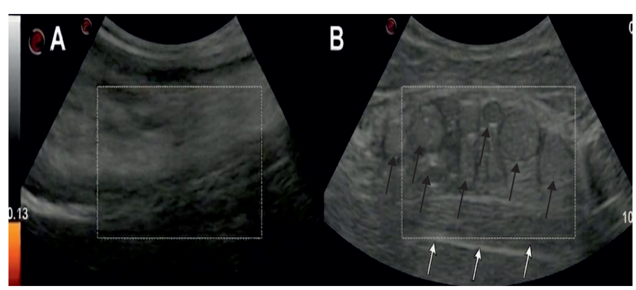

Fig 17. Ultrasound of the camel hump shows homogenous subcutaneous fat in control group (A), compared to hypoechoic/anechoic heterogeneous nodules of injected filler within thesubcutaneous fat (black arrow), causing localised thickening without muscle involvement or detectable vascular flow (white arrow) (B).

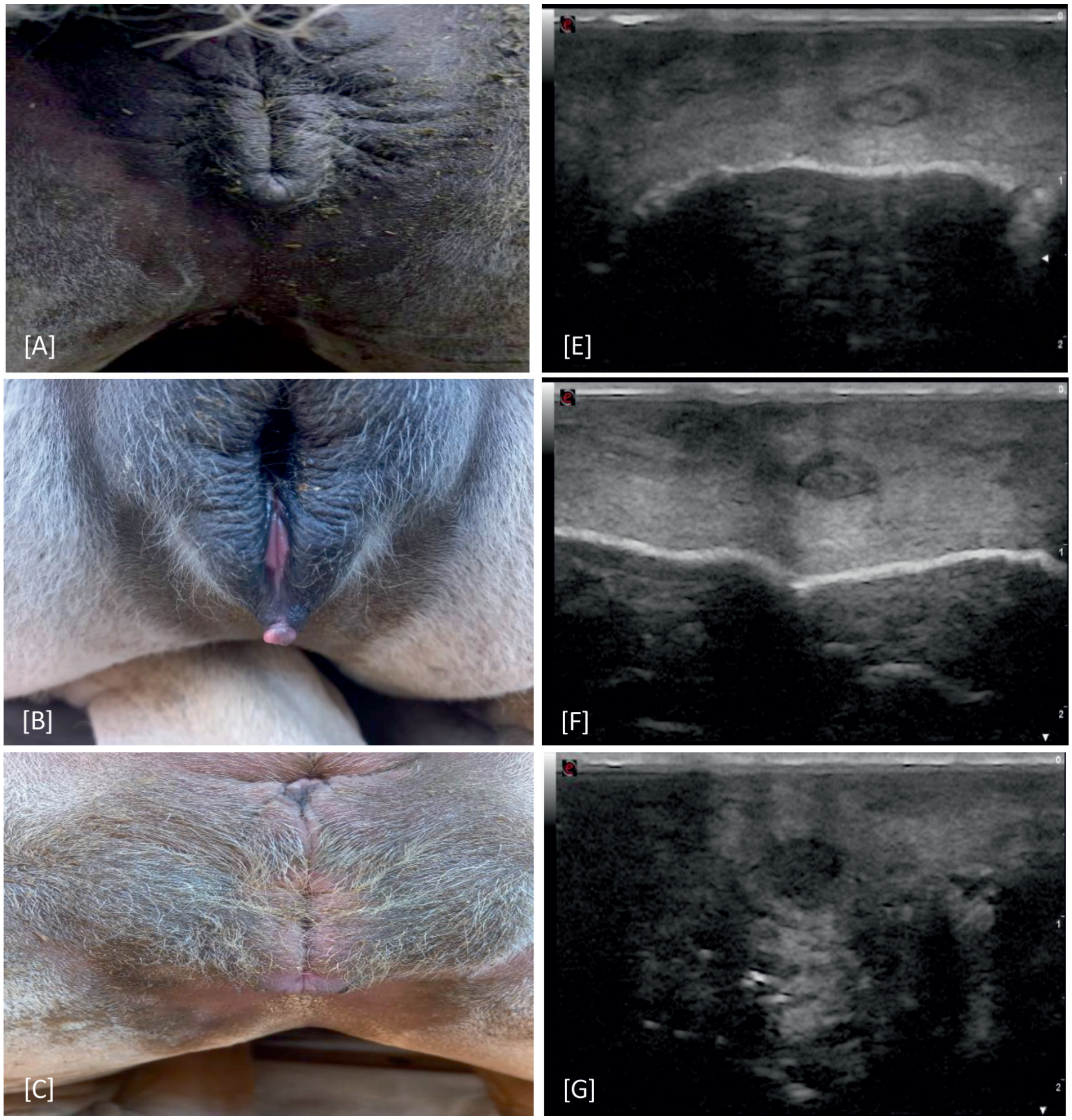

Fig 18. Visible clinical signs indicative of elevated testosterone levels (A) normal size and shape of clitoris; (B) enlarged and protruded clitoris; (C) partial cutting of external part of clitoris, with development of the dulla (white arrow) in a female camel (D). ultrasound of the female camel clitoris shows: (D) normal: small, homogeneous, well-defined, moderate echogenicity, normal vascular flow; (E) hormonally treated: enlarged, homogeneous, well-defined, mild protrusion/thickening of surrounding tissues; (F) severe cases: disrupted or partially absent tissue; (G) irregular heterogeneous hypoechoic/anechoic areas, ill-defined margins, localised thinning.

lips exhibited a lighter and more heterogeneous thermal pattern compared to the darker, homogeneous appearance of healthy lips (Fig 19).

With Infrared thermal camera the normal tissue of head and neck appeared as uniform warm colour (red-orange) with bilateral symmetrical pattern. While the injected animals by air showed irregular cool patches (blue-purple) temperatures than surrounding tissue with asymmetrical zones, often with sharp or unnatural edges in one-sided or localised swelling with temperature variation. While in cases that developed fluid buildup and abscess formation showed moderate to higher heat (red, orange or yellow rim around cooler area or white) (Fig 20).

Infrared thermography of normal female clitoris demonstrated a uniform thermal pattern, with temperatures comparable to surrounding tissues and no focal thermal anomalies. Whereas, infrared thermography of the clitoris in hormonally treated female camels revealed either pronounced protrusion appearing as a relatively darker, warmer area reflecting increased blood flow, or partial/ complete disruption showing irregular thermal patterns with mixed lighter and darker regions

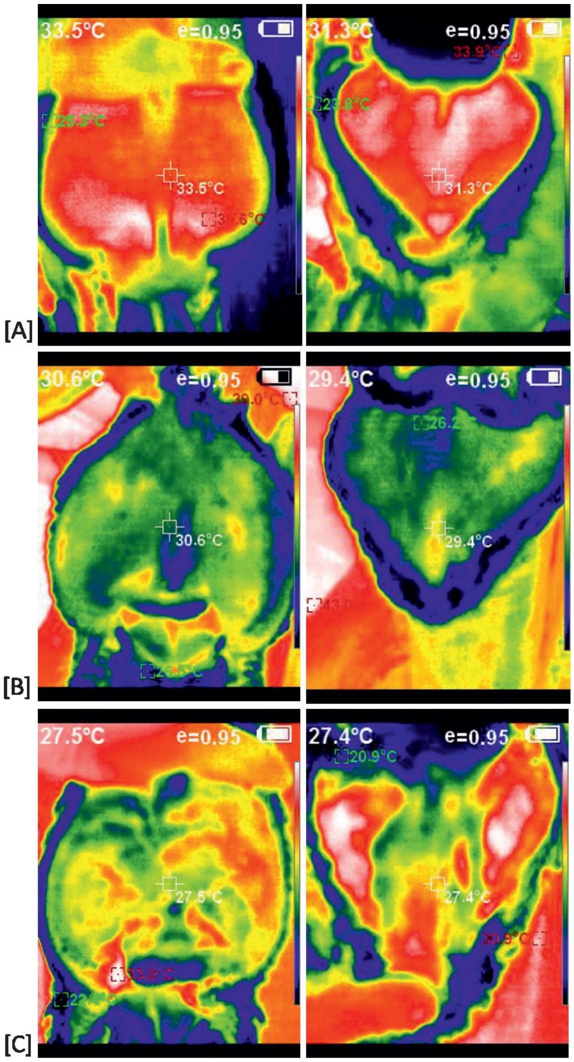

Fig 19. Infrared thermography (IRT) of the lips shows: (a) normal lips (upper and lower): dark, homogeneous thermal pattern; (b) injected filler sites: darker areas indicating relatively higher temperature than surrounding tissue; (c) stretched lips: lighter, heterogeneous thermal pattern compared to normal lips.

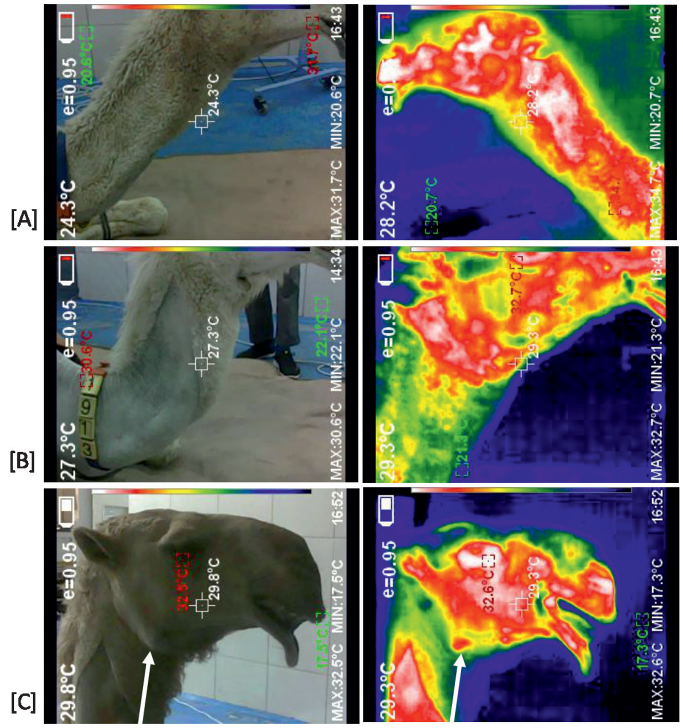

Fig 20. Infrared thermography of the head and neck shows: (a) normal tissue: uniform warm (red–orange), bilaterally symmetrical pattern; (b) air-injected cases: irregular cool patches (blue–purple), asymmetrical with sharp or localised edges; (c) abscess: moderate to high heat (red–orange–yellow rim) surrounding cooler or white areas.

corresponding to tissue loss and altered heat distribution (Fig 21).

Infrared thermographic examination of the camel hump revealed clear differences between normal and silicone-injected cases. In control animals, the hump exhibited a homogeneous and symmetrical thermal pattern, with uniform temperature distribution comparable to adjacent body regions, reflecting normal vascularisation and tissue integrity. In contrast, silicone-injected humps demonstrated heterogeneous and

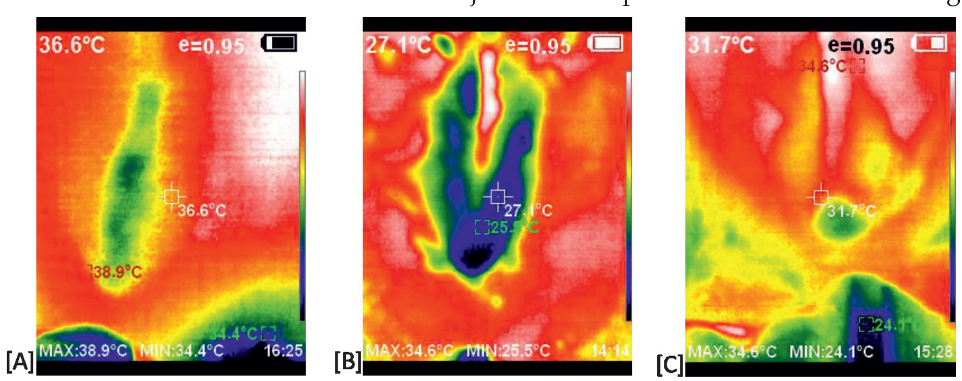

Fig 21. Infrared thermography of the female camel clitoris shows: (a) normal: uniform thermal pattern with no focal anomalies; (b) hormonally treated: protruded clitoris appearing as a darker, warmer area (increased blood flow); (c) severe cases: partial/complete disruption with irregular, heterogeneous thermal pattern (mixed lighter and darker areas).

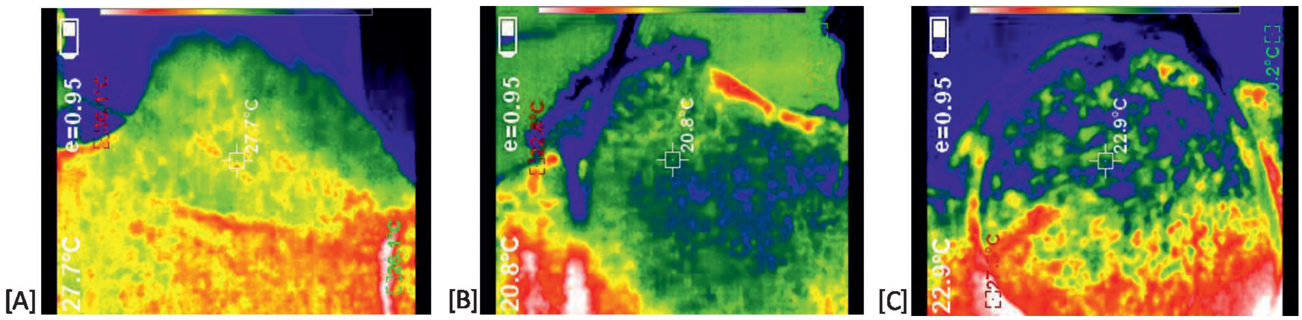

Fig 22. Infrared thermography of the camel hump shows: (A) normal: homogeneous, symmetrical thermal pattern with uniform temperature distribution; (B)silicone-injected: heterogeneous, asymmetrical pattern with focal hypothermic areas and occasional warmer zones; (C) advanced changes: thermally irregular contour with mixed temperature distribution, reflecting altered morphology and tissue reaction.

asymmetrical thermal patterns, characterised by focal areas of reduced temperature (hypothermic regions) interspersed with occasional localised warmer zones. The hypothermic areas likely correspond to the presence of silicone material, which has low thermal conductivity and limited vascular interaction, while the warmer regions may indicate localised inflammatory reactions or tissue irritation surrounding the injected material. Additionally, the overall contour of the hump appeared thermally irregular, correlating with the altered morphology and increased thickness observed clinically (Fig 22).

EMG of the camel lips

Electromyographic (EMG) assessment of lip muscles in camels revealed distinct patterns across the examined camels (Fig 23). In the control group, healthy lips with pathologically intact muscles exhibited spontaneous activity that was recorded and quantified as amplitude, with an average of 1.036 µV. In camels with stretched lips, spontaneous activity of the *M. Orbicularis Oris, M. Mentalis, M. Incisivus Superioris* and *M. IncisivusInferioris* was significantly reduced ($P < 0.05$) compared to the control group, with an average amplitude of 0.2 ± 0.15 µV, reflecting diminished neuromuscular function due to mechanical stretching. In camels whose lips were injected with filler materials, EMG recordings showed a further reduction in spontaneous muscle activity compared to the stretched lips group. The amplitudes were lower and more variable depending on the amount and location of the injected material. Conversely, lips subjected to local

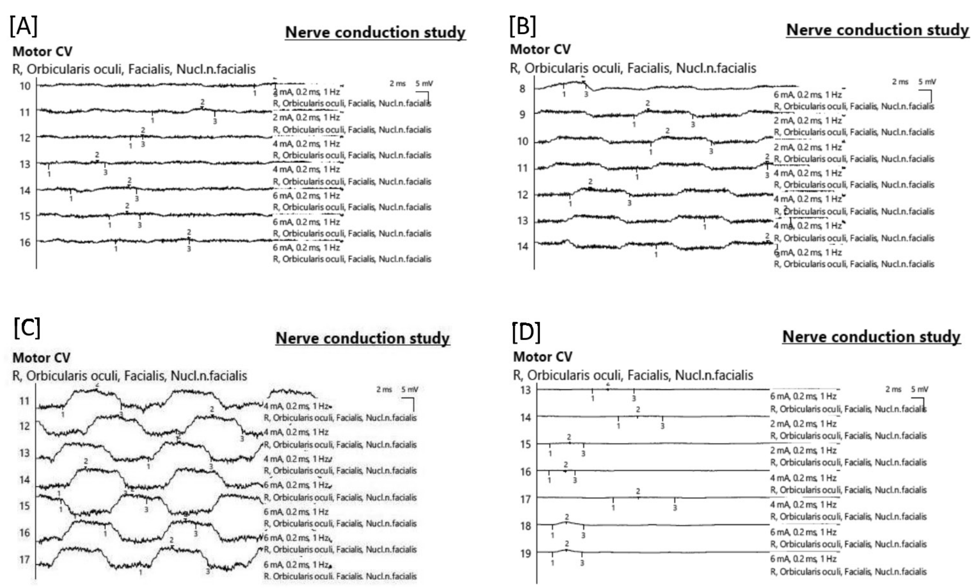

Fig 23. EMG of lip muscles in camels shows: (A) control: normal spontaneous muscle activity; (B) stretched lips: significantly reduced activity (low amplitude); (C) filler-injected: further reduced and variable activity; (D) local anaesthesia: near-complete suppression of activity (amplitude ≈ 0).

anaesthesia demonstrated near-complete suppression of spontaneous activity in all assessed muscles, with amplitudes approaching zero. This finding confirms effective blockage of neuromuscular transmission due to the anaesthetic agent, preventing voluntary or spontaneous muscle contractions.

Discussion

The present study provides a comprehensive evaluation of various forms of tampering in dromedary camels using multiple diagnostic imaging modalities (radiography, computed tomography, ultrasonography, infrared thermography) and electromyography (EMG), and offers insight into the prevalence, imaging characteristics, and neuromuscular consequences of these practices. Out of 5,365 camels examined, 20.4% were confirmed to have undergone some form of tampering, with lip stretching being the most prevalent method recorded, followed by air injection in head and neck region, nasal injection with fillers, signs of elevated testosterone, and lip binding. Less frequently observed manipulations included lip filler injection, nostril abscessation, ear cropping, nerve anaesthesia, and hump filler injection.

Consistent with previous reports from large-scale surveys at camel beauty festivals, stretching of the lips and perinasal filler injections represent major forms of cosmetic manipulation in camels and can be reliably detected using clinical examination supported by diagnostic imaging techniques. Ultrasonography has been shown to precisely discriminate between normal and manipulated tissues, with injected fillers appearing as hypoechoic or anechoic foci in both the lips and perinasal region, corroborating earlier findings in similar camel populations (Tharwat *et al*, 2024).

Radiographically, the presence of air pockets in the soft tissues of the throat and neck produced diffuse radiolucent areas in acute stages, whereas chronic or complicated cases with secondary infection exhibited soft tissue opacities and calcifications, reflecting progressive tissue reaction and fibrosis. These findings align with reports that soft tissue alterations due to fillers may exhibit heterogeneous densities on X rays, potentially influenced by filler composition and quantity (Ouyang and Branstetter, 2010; Scrivani, 2022; Tharwat and Al-Hawas, 2025). Although, radiographic density varies with filler type, previous work also emphasises the variable radiographic appearance of dermal fillers based on composition (Valiyaparambil *et al,* 2009), supporting our interpretation that hyaluronic acid derivatives may present differently from other compounds. Radiographic assessment of the camel hump revealed distinct differences between normal and filler-injected cases. Normal humps showed homogeneous soft tissue opacity reflecting intact tissue architecture, while injected humps exhibited focal to multifocal radiopaque areas with irregular margins and heterogeneous internal patterns, corresponding to the presence and variable distribution of exogenous materials, sometimes causing contour irregularities and localised enlargement, consistent with cosmetic augmentation (Kwon *et al,* 2018; Valiyaparambil *et al,* 2009). Variations in radiographic appearance are influenced by filler composition, such as silicone, calcium-based compounds, or hyaluronic acid derivatives, producing different radiodensity profiles, as reported in both veterinary and human imaging studies (Alsufyani *et al,* 2022; Mundada *et al,* 2017).

CT imaging further delineated the anatomical changes associated with tampering. In animals with stretched lips, binding lips, tissue tearing and oedema manifested as hypodense regions within the dermis, whereas filler materials appeared as well defined hyperdense deposits within submucosal and subcutaneous layers. The variations in attenuation and architectural disruption seen on CT scans reflect the diverse physical properties of injected materials in lips and perinasal region and the degree of associated soft tissue reaction, observations that are also described in the limited literature on filler imaging in both veterinary and human medicine (Alsufyani *et al,* 2022; Nahas *et al,* 2024; Rubinstein *et al,* 1996). The observed CT attenuation differences in tissues with oedema, fat plane disruption, and filler nodules align with known imaging features of foreign material deposition in soft tissue, similar to reports of dermal fillers presenting radiographically as distinct densities (Kwon *et al,* 2018; Mundada *et al,* 2017). CT examination of the camel cervical region showed normal soft tissue and fat distribution in controls, while injected cases exhibited low-attenuation areas, irregular contours, and occasional diffuse soft tissue density changes due to fluid accumulation and oedema (Alsufyani *et al,* 2022; Kwon *et al,* 2018; Valiyaparambil *et al,* 2009). These findings indicate that CT effectively detects exogenous material and associated tissue alterations. CT imaging of the camel hump revealed normal uniform low-attenuation fat in controls, whereas injected cases showed focal or multifocal hyperattenuating deposits with irregular margins, heterogeneous internal structure, and occasional contour deformities, reflecting exogenous filler presence (Lee *et al,* 2022; Mundada *et al,* 2017). These findings confirm that CT effectively detects both filler material and associated soft tissue alterations.

Ultrasonography proved valuable in delineating filler material as hypoechoic or anechoic foci, and in identifying additional soft tissue abnormalities such as oedema and fluid accumulation. This aligns with early veterinary studies that first documented the utility of ultrasound for localising cosmetic filler injections in camel lips and perinasal region, highlighting a pattern of heterogeneous echotexture and variable echogenicity (Marzok *et al,* 2025; Tharwat and Al-Hawas, 2021; Young *et al,* 2008). Ultrasonography can detect hyperechoic foci with posterior dirty shadowing, corresponding to gas within soft tissues, and is useful for identifying both gas collections and inflammatory changes in soft tissue infections. This has been demonstrated in sonographic evaluations of necrotising soft tissue infections in cervical region, where gas pockets and fluid collections produce characteristic artifacts and echogenic patterns on real time ultrasound (Butcher *et al,* 2011; Gan *et al,* 2023; Nahas *et al,* 2024; Wortsman and Wortsman, 2011; Yoo, 2024). Ultrasonographic assessment in the present study revealed distinct differences between normal and filler treated tissues. In controls, the hump subcutaneous and fatty layers demonstrated typical soft tissue echotexture, whereas injected filler material appeared as hypoechoic or anechoic heterogeneous nodules with irregular distribution and localised thickening, consistent with documented ultrasound patterns of dermal fillers (e.g., anechoic/hypoechoic filler deposits and mixed echotexture seen on high frequency US) in human imaging studies (Chiang and Liao, 2025; Urdiales-Gálvez *et al,* 2021). Similarly, normal camel clitoris exhibited a small, homogeneous structure with uniform echogenicity and normal Doppler flow, while hormonally altered clitoral tissue showed pronounced enlargement or disrupted heterogeneous hypoechoic/anechoic areas, reflecting alterations in tissue architecture analogous to pathological changes described in soft tissue ultrasonography (Thomaz *et al,* 2026). Overall, these findings support the utility of ultrasound for identifying exogenous material and associated soft tissue alterations in both hump and genital regions.

Infrared thermography (IRT) offered additional functional information. Normal head and neck tissues exhibited uniform thermal symmetry, whereas injected or stretched regions showed thermal asymmetry, cooler or hotter areas, and heterogeneous patterns. When assessing a thermal image, asymmetry of 1°C or more is often significant and indicates possible pathology. The darker thermal signatures of injected lips observed in our study indicating relatively higher local temperature likely reflect superficial inflammation, consistent with thermographic findings described in camels with injected or stretched lips (Redaelli *et al,* 2014; Schaefer *et al,* 2004; Stelletta *et al,* 2012; Tharwat, 2025; Tharwat *et al,* 2021). Infrared thermography proved useful in differentiating normal from silicone-augmented humps. The uniform thermal distribution observed in normal camels reflects intact vascular perfusion and consistent tissue composition. In contrast, silicone injection resulted in disrupted thermal patterns, with predominantly hypothermic areas due to the insulating properties of silicone and its lack of metabolic activity. The presence of adjacent hyperthermic zones may be attributed to secondary inflammatory responses or altered local blood flow. These findings are consistent with previous studies demonstrating that infrared thermography is sensitive to variations in tissue perfusion and inflammatory processes, where hyperthermic regions are associated with increased blood flow and inflammation, while hypothermic areas may reflect reduced vascularity or the presence of non-biological materials (Brothers *et al,* 2025; Stelletta *et al,* 2012). Moreover, the altered thermal distribution observed in silicone-injected tissues of hump aligns with reports describing the impact of foreign materials on local heat patterns and tissue physiology (Ring and Ammer, 2012). Collectively, these findings highlight the sensitivity of IRT in detecting subtle physiological alterations associated with cosmetic tampering and support its role as a non-invasive diagnostic tool in field conditions. Infrared thermography in this study effectively distinguished normal from altered clitoral tissue patterns. Normal clitorises exhibited a uniform thermal distribution without focal anomalies, whereas hormonally treated animals showed areas of increased surface temperature corresponding to protrusion and enhanced blood flow, as well as irregular mixed thermal zones reflecting tissue disruption and altered heat distribution. These findings are consistent with previous thermographic studies demonstrating that changes in vascularity and soft tissue integrity produce measurable thermal pattern alterations, with warmer regions indicating increased perfusion or inflammation and heterogeneous patterns associated with structural disruption (Chava *et al,* 2023; Whittaker *et al,* 2023; Xu *et al,* 2025).

Electromyography (EMG) is a sophisticated electrodiagnostic-neurophysiological method, which serves to diagnose neuromuscular system diseases which may be due to using a local anaesthetic, either in the form of injections or ointments, to induce laxity in the lips is one of the methods of tampering in camels, as it leads to the drooping of the lower lip and changing the appearance of the camel. It is based on the measurement of the electrical potentials created by the skeletal muscle activity. From a neurophysiological standpoint, EMG recordings revealed a progressive decline in spontaneous muscle activity from control camels to those with stretched or filler injected lips, and near complete suppression in locally anaesthetised animals. This pattern is biologically plausible given the impact of mechanical stress on neuromuscular recruitment and the inhibitory effect of local anaesthetics on nerve conduction. Local anaesthetics block voltage gated sodium channels, preventing action potential propagation and resulting in significantly reduced EMG activity in anaesthetised muscles compared with control and stretched conditions (Strichartz, 1976). Clinical studies have demonstrated that regional nerve blocks markedly suppress motor nerve conduction and EMG amplitudes, consistent with our findings of near complete EMG suppression in locally anaesthetised lip muscles (Byram *et al,* 2020; Luo *et al,* 2020). Although, direct veterinary EMG comparisons are limited, similar trends have been documented in the assessment of facial muscles following cosmetic interventions in human patients, where fillers and neuromuscular modifiers alter baseline electrophysiological activity (Tharwat and Al-Hawas, 2025).

This study provides comprehensive clinical and diagnostic evaluation of various cosmetic enhancements in camels, including lips stretching, lips binding, injection of the lips and nose by a filler material, visible clinical signs indicative of elevated testosterone levels.

The findings clearly demonstrated the substantial health risks and significant welfare concerns associated with various cosmetic enhancements, reinforcing the introduction's assertion regarding these dangers. Notably, this study documents severe tissue damage, inflammation, functional impairment, and long-term structural alterations, particularly in the chronic cases of air injection and the widespread use of fillers. These abnormalities constitute direct evidence of the suffering inflicted upon the animals, justifying the rigorous implementation of diagnostic examinations to not only eliminate cheating and ensure fair competition but also, crucially, to safeguard the welfare and health of camels.

Clinically, this multidimensional approach enhances detection sensitivity and aids in differentiating between recent versus chronic manipulations, inflammatory versus non inflammatory changes, and mechanical versus pathological tissue alterations. This integrated protocol represents a comprehensive diagnostic approach, as each modality is capable of detecting specific forms of cosmetic tampering; therefore, its combined application ensures that no form of manipulation or fraud in camels can go undetected.

Acknowledgements

We extend our sincere gratitude to Mr. Fhad El-Fhad, Chairman of the Board of Directors of Salam Veterinary Group, and to Mr. Saleh Al-Tuwayjiri, CEO of Salam Veterinary Group, for their insightful guidance, continuous encouragement, and for facilitating the essential resources that made this research possible.

Our appreciation is also due to the administrative staff and the herd managers of Salam Veterinary Group for their generous support and invaluable assistance throughout the course of this work.

Author contribution

The authors confirm contribution to the paper as follows: study conception and design, data collection, analysis and interpretation of results and draft manuscript preparation: Ellawatty WAE. Margreet V. and Ellawatty WAE. reviewed the results and approved the final version of the manuscript.

Funding

This research received no external funding.

Institutional Review Board Statement

This is a retrospective study conducted in a commercial medical imaging centre in the 2020–2026. All of the procedures were approved by the local ethical committee of Salam Camel Hospital, Salam Veterinary Group, Co., Qassim, Saudi Arabia (Approval code: SVG 0316202237).

Informed Consent Statement

Not applicable.

Data Availability Statement

Data availability is possible upon request.

Conflicts of Interest

Author Waleed Elsayed Ahmed Ellawatty was employed by the company Medical Imaging Department, Salam Veterinary Group Co. The remaining author declare that the research was conducted in the absence of any commercial or financial relationships that could be construed as a potential conflict of interest.

References

Ahmad S, Yaqoob M, Hashmi N, Ahmad S, Zaman M and Tariq M. Economic importance of camel: unique alternative under crisis. Pakistan Veterinary Journal. 2010; 30(4):191–197.

Al-Mubarak A, Abdin-Bey M and Ramadan R. A retrospective clinical evaluation of xylazine-ketamine total intravenous anaesthesia (TIVA) in dromedary camels. Journal of Camel Practice and Research. 2008; 15:201-203.

Alsufyani N, Aldosary R, Alrasheed R and Alsufyani M. Clinical and radiographic features of facial cosmetic materials: a systematic review. Imaging Science in Dentistry. 2022; 52(2):155-164. https://doi.org/10.5624/isd.20210292

Bieh K, ElGanainy A, Yezli S, Malik M, Jokhdar HA, Asiri A and Alotaibi B. Health risk assessment at mass gatherings: a report of the camel festival in Saudi Arabia. Eastern Mediterranean Health Journal. 2019; 25(9):647-655. https://doi.org/10.26719/emhj.18.071

Brothers NI, Rebman A, Zenilman JM and Aucott J. Use of Infrared Thermography in visualising erythema Migrans. Cureus. 2025; 17(8):e89242. https://doi.org/10.7759/cureus.89242

Butcher CH, Dooley RW and Levitov AB. Detection of subcutaneous and intramuscular air with sonography: a sensitive and specific modality. Journal of Ultrasound in Medicine. 2011; 30(6):791-795. https://doi.org/10.7863/jum.2011.30.6.791

Byram SC, Bialek SE, Husak VA, Balcarcel D, Park J, Dang J and Foecking EM. Distinct neurotoxic effects of select local anaesthetics on facial nerve injury and recovery. Restorative Neurology and Neuroscience. 2020; 38(2):173-183. https://doi.org/10.3233/rnn-190987

Chava SK, Agrawal M, Vidya K, Janakiraman R, Palaniyandi K, Ramachandran O and Tirkey AJ. Role of infrared thermography in planning and monitoring of head and neck microvascular flap reconstruction. Plastic and Reconstructive Surgery - Global Open. 2023; 11(9):e5158. https://doi.org/10.1097/gox.0000000000005158

Chiang J and Liao YH. Mapping Filler Nodules: Ultrasound characteristics and clinical patterns in dermal filler complications. Dermatologic Surgery. 2025. https://doi.org/10.1097/dss.0000000000004963

Gan RK, Sanchez Martinez A, Abu Hasan MA, Castro Delgado R and Arcos González P. Point-of-care ultrasonography in diagnosing necrotising fasciitis-a literature review. Journal of Ultrasonography. 2023; 26(2):343-353. https://doi.org/10.1007/s40477-022-00761-5

Kwon YE, An CH, Choi KS, Lee DH and An SY. Radiographic study of dermal fillers in the facial area: A series of 3 cases. Imaging Science in Dentistry. 2018); 48(3):227-231. https://doi.org/10.5624/isd.2018.48.3.227

Lee C, Choi YJ, Jeon KJ, Choi SH and Han SS. Imaging feature of cosmetic fillers in cone-beam computed tomography and its dental consideration. Head and Face Medicine. 2022; 18(1):24. https://doi.org/10.1186/s13005-022-00327-0

Luo J, Cai G, Ling D, Zhang N, Chen X, Cao X and Yu B. Mean effective volume of local anaesthetics by nerve conduction technique. Annals of Translational Medicine. 2020; 8(5):174. https://doi.org/10.21037/atm.2020.01.96

Marzok M, Hussen J, Al Dhafiri M, Saleh S, El-Husseiny HM, El-Sherif MW, Ayman Al Wail A, Almubarak AI and Salem M. Ultrasound assessment of botulinum toxin-A (BOTOX) injection into adult Arabian dromedary camels' lips: efficacy in detection and localisation. BMC Veterinary Research. 2025; 21(1):336. https://doi.org/10.1186/s12917-025-04757-1

Mundada P, Kohler R, Boudabbous S, Toutous Trellu L, Platon A and Becker M. Injectable facial fillers: imaging features, complications and diagnostic pitfalls at MRI and PET CT. Insights Imaging. 2017; 8(6):557–572. https://doi.org/10.1007/s13244-017-0575-0

Nahas AE, Almohamad Z and Hagag U. Ultrasonography, computed tomography and magnetic resonance imaging of the dromedary camel distal limbs. BMC Veterinary Research. 2024; 20(1):12. https://doi.org/10.1186/s12917-023-03855-2

Ouyang T and Branstetter BFt. Advances in head and neck imaging. Oral and Maxillofacial Surgery Clinics of North America. 2010; 22(1):107-115. https://doi.org/10.1016/j.coms.2009.10.002

Redaelli V, Tanzi B, Luzi F, Stefanello D, Proverbio D, Crosta L and Di Giancamillo M. Use of thermographic imaging in clinical diagnosis of small animal: preliminary notes. Ann Ist Super Sanita. Annali dell'Istituto Superiore di Sanità. 2014; 50(2):140-146. https://doi.org/10.4415/ann_14_02_06

Ring EF and Ammer K. Infrared thermal imaging in medicine. Physiological Measurement. 2012; 33(3):R33-46. https://doi.org/10.1088/0967-3334/33/3/r33

Rubinstein D, Dangleis K and Damiano TR. Venous air emboli identified on head and neck CT scans. Journal of Computer Assisted Tomography. 1996; 20(4):559-562. https://doi.org/10.1097/00004728-199607000-00011

Schaefer A, Cook N, Tessaro S, Deregt D, Desroches G, Dubeski P, Tong A and Godson D. Early detection and prediction of infection using infrared thermography. Canadian Journal of Animal Science. 2004; 84(1):73-80.

Scrivani P. Veterinary Head and Neck Imaging. 2022. https://doi.org/10.1002/9781119118633

Stelletta C, Gianesella M, Vencato J, Fiore E and Morgante M. Thermographic applications in veterinary medicine. Infrared Thermography. 2012; 13:117-140.

Strichartz G. Molecular mechanisms of nerve block by local anaesthetics. Anaesthesiology. 1976; 45(4):421-441. https://doi.org/10.1097/00000542-197610000-00012

Tharwat M. Cosmetic crimes in dromedary camels: a critical overview on these illegal manipulations and its hidden consequences. Frontiers in Veterinary Science. 2025; 12:1632022. https://doi.org/10.3389/fvets.2025.1632022

Tharwat M and Al-Hawas A. Ultrasound detection of cosmic filler injection of lips in camel beauty pageants: first report in veterinary medicine. Tropical Animal Health and Production. 2021; 53(1):53. https://doi.org/10.1007/s11250-020-02551-9

Tharwat M and Al-Hawas A. Identification of tampering methods among 12,385 Arabian camels using different diagnostic imaging techniques. Open Veterinary Journal. 2025; 15(3):1226-1238. https://doi.org/10.5455/OVJ.2025.v15.i3.14

Tharwat M, Al-Hawas A and Alboti Y. Infrared thermography in dromedary camels with injected and stretched lips in camel beauty pageants. Journal of Camel Practice and Research. 2021; 28(3):355-359.

Tharwat M, Sadan M and Al-Hawas A. The emerging topic of injected cosmetic fillers in the perinasal region of dromedary camels: ultrasonographic and radiographic verification. Open Veterinary Journal. 2024; 14(3):840-845. https://doi.org/10.5455/OVJ.2024.v14.i3.11

Thomaz MFR, Klassen AV, Rothenburg IT, Bertani TD, Abrantes BLA, Freitas CFd, Arita ES, Watanabe PCA, Silva Yd, Munhoz L and Cordasso GC. Facial dermal filler imaging features in ultrasonography: An illustrated systematic review and a guideline for filler identification. Revista de Medicina. 2026; 105(1):e–235693. https://doi.org/10.11606/issn.1679-9836.v105i1e-235693

Urdiales-Gálvez F, De Cabo-Francés FM and Bové I. Ultrasound patterns of different dermal filler materials used in aesthetics. Journal of Cosmetic Dermatology. 2021; 20(5):1541-1548. https://doi.org/10.1111/jocd.14032

Valiyaparambil J, Rengasamy K and Mallya SM. An unusual soft tissue radiopacity – radiographic appearance of a dermal filler. British Dental Journal. 2009; 207(5):211-212. https://doi.org/10.1038/sj.bdj.2009.764

Whittaker AL, Muns R, Wang D, Martínez-Burnes J, Hernández-Ávalos I, Casas-Alvarado A, Domínguez-Oliva A and Mota-Rojas D. Assessment of pain and inflammation in domestic animals using infrared thermography: a narrative review. Animals. 2023; 13(13):2065.

Wortsman X and Wortsman J. Sonographic outcomes of cosmetic procedures. American Journal of Roentgenology. 2011; 197(5):W910–918. https://doi.org/10.2214/ajr.11.6719

Xu Y, Xu M, Huang P, Zhu Q, Jiang X and Cai F. Infrared thermography for assessing skin temperature characteristics of postoperative blanching erythema and stage 1 pressure injuries. Journal of Tissue Viability. 2025; 34(4):100963. https://doi.org/https://doi.org/10.1016/j.jtv.2025.100963

Yoo JH. Ultrasonographic findings of complications related to cosmetic procedure. Ultrasound in Medicine and Biology. 2024; 50:S22–S24. https://doi.org/https://doi.org/10.1016/j.ultrasmedbio.2024.01.036

Young SR, Bolton PA and Downie J. Use of high-frequency ultrasound in the assessment of injectable dermal fillers. Skin Research and Technology. 2008; 14(3):320-323. https://doi.org/10.1111/j.1600-0846.2008.00297.x